iScience, Volume *26*

Supplemental information

Single cell RNA sequencing unravels mechanisms underlying senescence-like phenotypes of alveolar macrophages

Yue Wu, Shengen Shawn Hu, Ruixuan Zhang, Nick P. Goplen, Xiaochen Gao, Harish Narasimhan, Ao Shi, Yin Chen, Ying Li, Chongzhi Zang, Haidong Dong, Thomas J. Braciale, Bibo Zhu, and Jie Sun

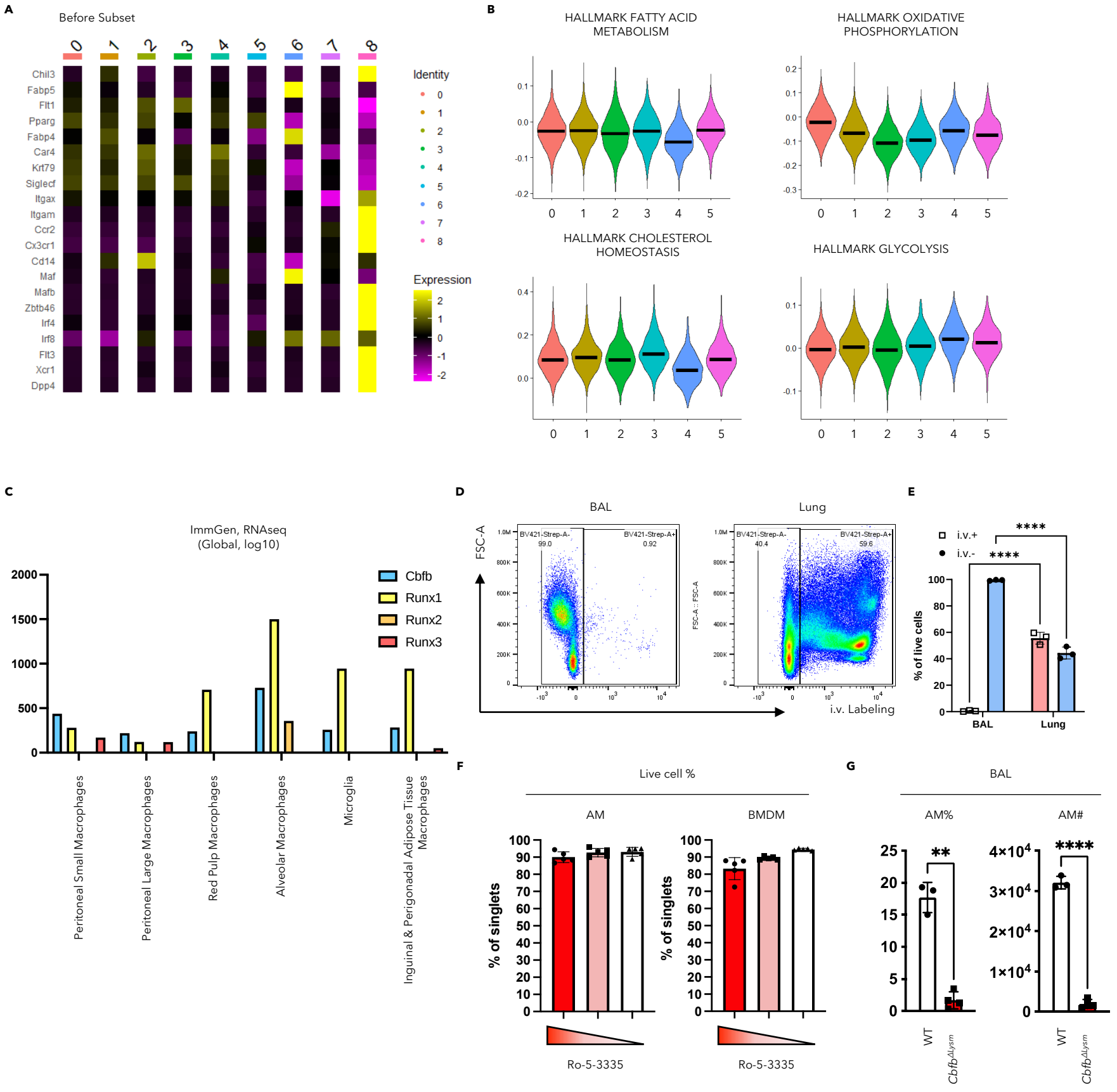

Figure S1 Characterization of the transcriptome and the role of Cbfβ in AMs, related to Figure 1 and Figure 2.

A. Heatmap displaying average expression level of markers distinguishing AMs from other contaminating myeloid cells in the scRNAseq data before sub-setting AMs. **B.** Violin plots demonstrating module scores of genes lists for cellular metabolism with respect to the clusters shown in **Figure1 B**. **C.** Expression level of *Cbfb*, *Runx1*, *Runx2*, and *Runx3* using data from ImmGen. **(D. and E.)** To address the contamination of immune cells from blood in BAL, α-CD45 antibody was injected intravenously 5 minutes before sacrificing the wild type C57BL/6 mice. The vasculature associated immune cells were then evaluated with flow cytometry in BAL and lung single cell suspension. Representative FACS plot **(D)** and quantification **(E)** of vasculature-associated immune cells were shown. **F.** Percentage of live cells of AMs or BMDMs upon *in vitro* treatment of different doses of Ro 5-3335 (100μM, 50μM, and 0 μM respectively, each dot represents one biological replicate). **G.** Quantification of percentage and absolute number of AMs in the BAL in bone marrow chimera mice with bone marrow from *Cbfb*$^{\Delta Lysm}$ (n=3) or WT (n=4) mice.

Unpaired student t test with Welch's correction **(G)** was utilized for statistical evaluation. Data were shown as mean ± SD. **, p < 0.01; ****, p<0.0001. The bar in **(B)** represents the median of module scores generated with gene lists indicated among the cells in each cluster as shown in **(Figure 1B)**.

Supplementary Figure 2

A Before Sub-setting

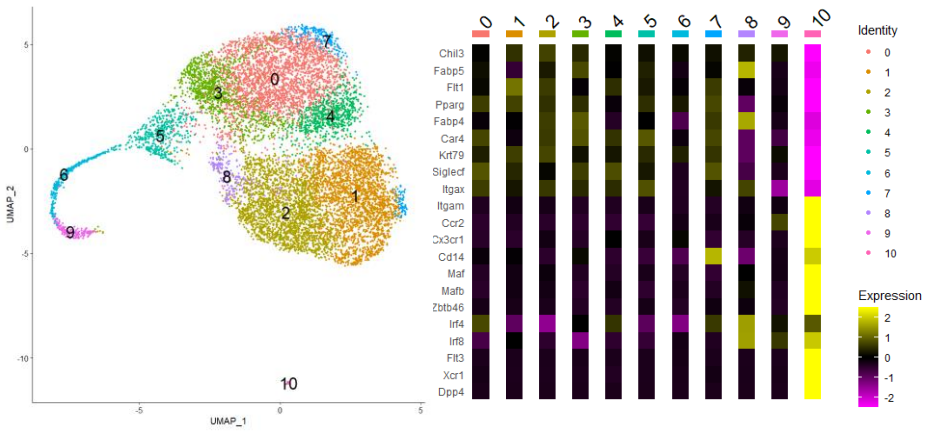

B GSE124872

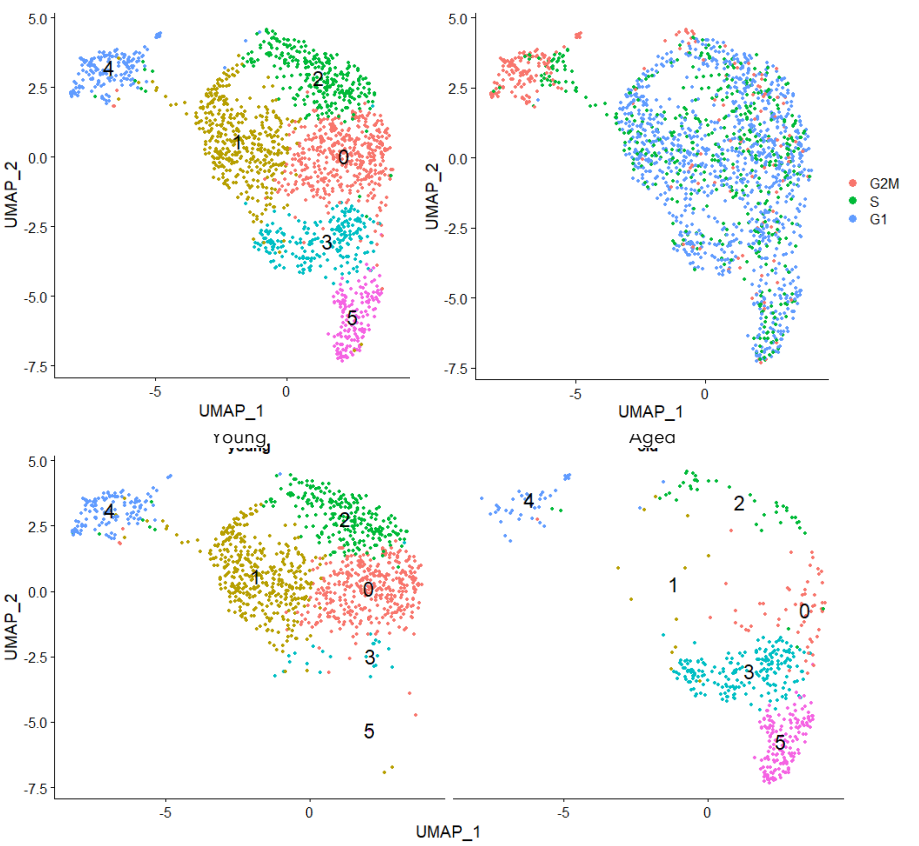

C GSE124872

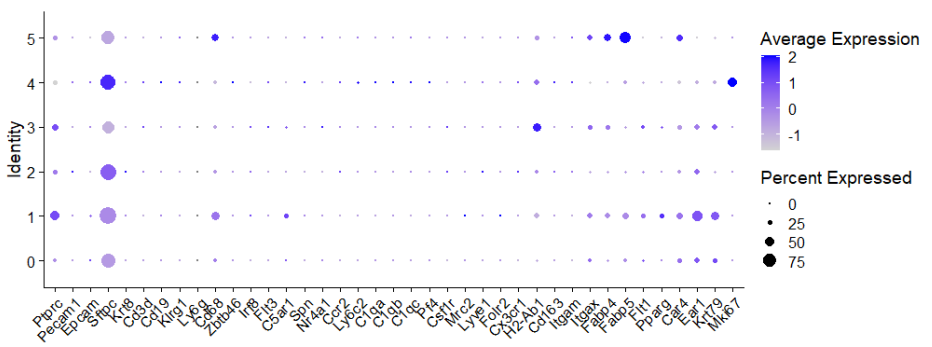

D

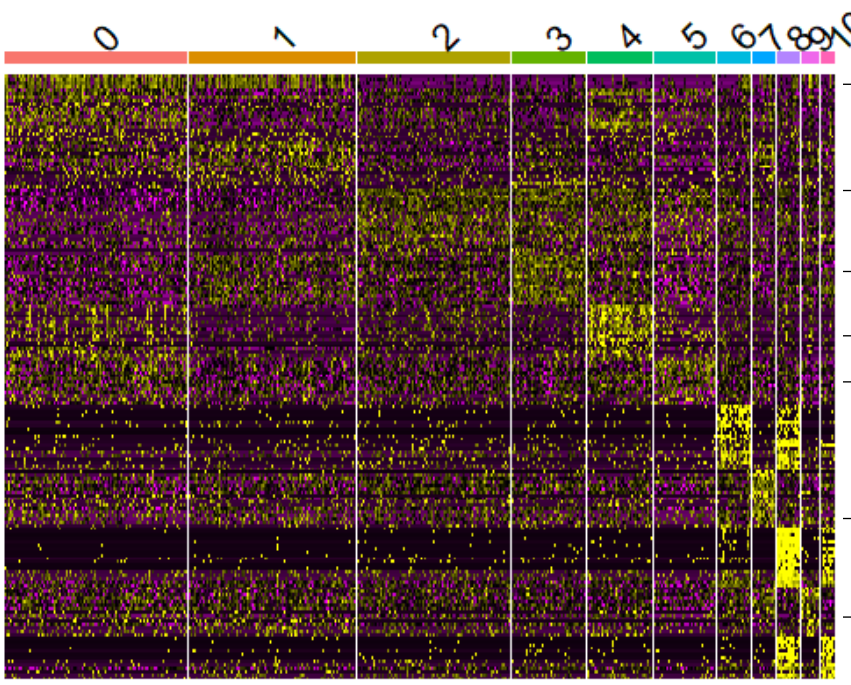

Cluster 0 and 1 (antigen-presenting)

H2-Eb1, H2-Ab1, H2-Aa, H2-DMb1, CD74, B2m

Cluster 2, 3 and 4

Fpr2, Gmfg, Fth1
Mgst3

Cluster 3 (intermediate)

Fcer1g, Tyrobp
Usmg5, Uqcrb, Ndufa4, Cox5a
Bcl2a1b, Bcl2a1d

Cluster 0 and 4 (poised inflammatory)

Fos, Fosb, Jun, Junb, Il1a, Il1b, Tnf, Cxcl1, Cxcl2, Cxcl3…
Nfkbia, Nfkbiz, Tnfaip3, Ier2

Cluster 5 (dying?)

Actb, Cap1, Ppt1, mt-Atp8

Cluster 7 & 9 (baseline/ surfactant turnover)

Psap, Ctsk, Lipa, Prdx, Fabp4, Fabp5, Gpnmb, Gstm1

Cluster6 (S phase)

Cluster8 & 10 (G2M phase)

E

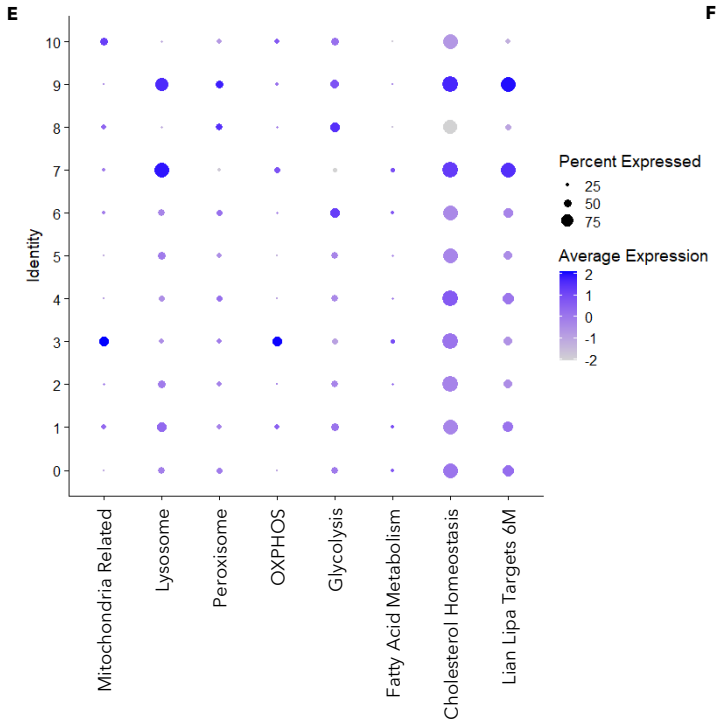

F

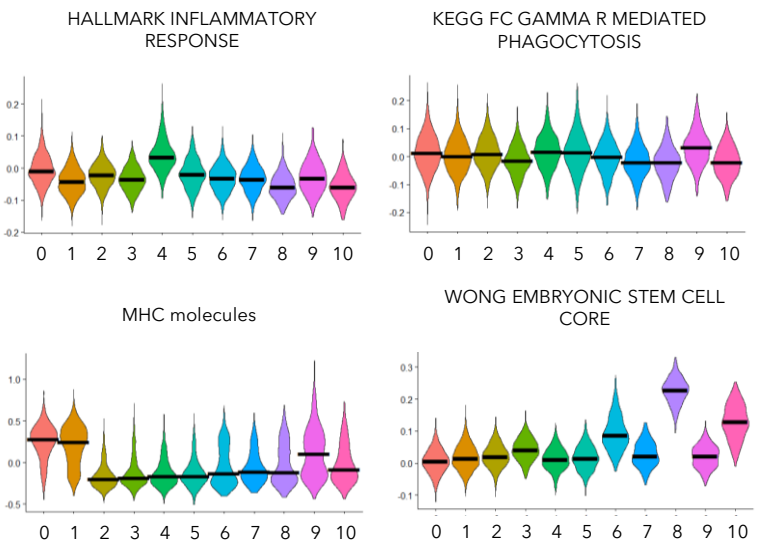

G

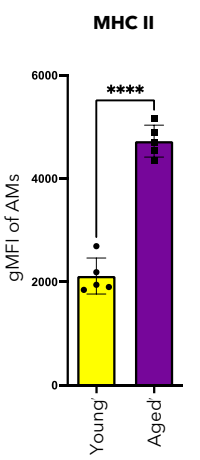

Figure S2 ScRNAseq reveals heterogeneity of AMs from young and aged mice, related to Figure 3.

A. Demonstration of clustering of cells before sub-setting. **(left)** UMAP displaying all cells that past quality control; **(right)** Heatmap revealing markers to distinguish AMs from other contaminating myeloid cells in the scRNAseq data. (**B-C)** AMs in scRNAseq dataset from GSE124872. **B.** UMAP displaying all AMs **(upper left)**, AMs by group **(lower)** and cell cycle analysis **(upper right)**. **C.** Dot Plot showing the markers for identification of AMs. **D.** Heatmap showing top 50 genes featured in each cluster (shown in **Figure 3B**) with selected genes shown on the right. **E.** Dot plot demonstrating module scores evaluating selected gene lists. **F.** Violin plots exhibiting module scores of selected gene lists of inflammatory response (MSigDB M5932), phagocytosis (MSigDB M16121), MHC molecules and ESC-like features (MSigDB M7079) in each cluster. **G.** Geometry mean fluorescence intensity (gMFI) of MHC II molecules in AMs from young (n=5) and aged (n=5) mice evaluated by flow cytometry.

Unpaired student t test with Welch's correction **(G)** was utilized for statistical evaluation. Data were shown as mean ± SD. ****, $p<0.0001$. The bar in **(F)** represents the median of module scores generated with gene lists indicated among the cells in each cluster as shown in **(Figure 3B)**.

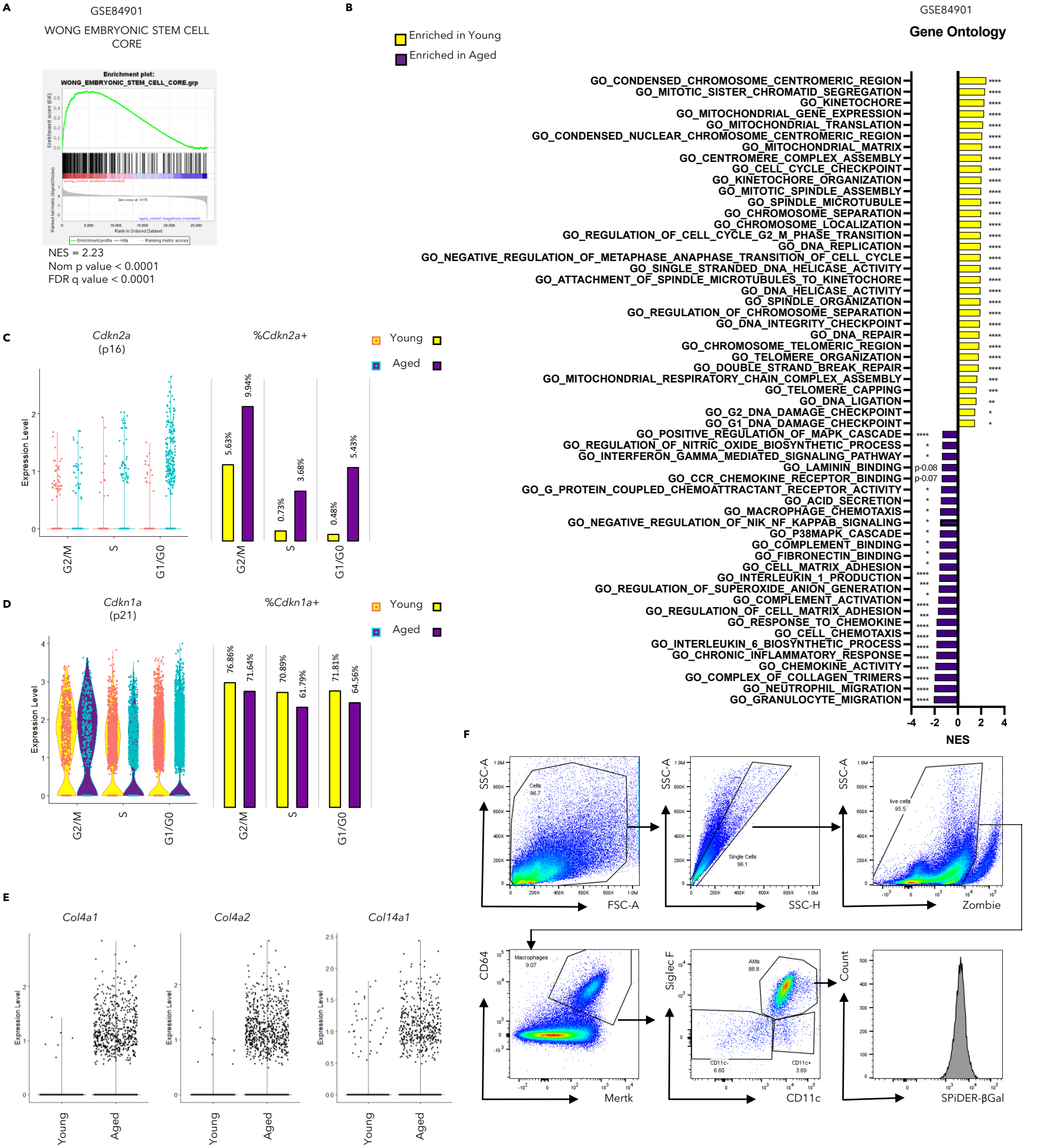

Figure S3 Pathway analysis revealed senescence-like phenotypes in AMs from aged mice, related to Figure 3 and Figure 4.

A. GSEA comparing the ESC like features (MSigDB M7079) of AMs from young and aged mice in published microarray data (GSE84901). **B.** Bar graph showing selected pathway analysis results using gene lists from Gene Ontology comparing AMs from young and aged mice with microarray data (GSE840901). **C.** Evaluation of *Cdkn2a* in scRNAseq dataset of AMs from young and aged mice with respect to cell cycle. **(left)** Violin Plot displaying expression of *Cdkn2a*. **(right)** Bar graph showing the proportion of *Cdkn2a*-expressing cells. **D.** Evaluation of *Cdkn1a* in scRNAseq dataset of AMs from young and aged mice with respect to cell cycle. **(left)** Violin Plot displaying expression of *Cdkn1a*. **(right)** Bar graph showing the proportion of *Cdkn1a*-expressing cells. **E.** Violin plots comparing the mRNA expression for Collagen IV and XIV in AMs from young and aged mice. **F.** Representative plot demonstrating the gating strategy for SPiDER-βGal staining in AMs demonstrated in **Figure 4F**.

Data were analyzed with GSEA **(A and B)**. Data were shown as mean ± SD. *, p<0.05; **, p < 0.01; ***, p<0.001; ****, p<0.0001.

Supplementary Figure 4

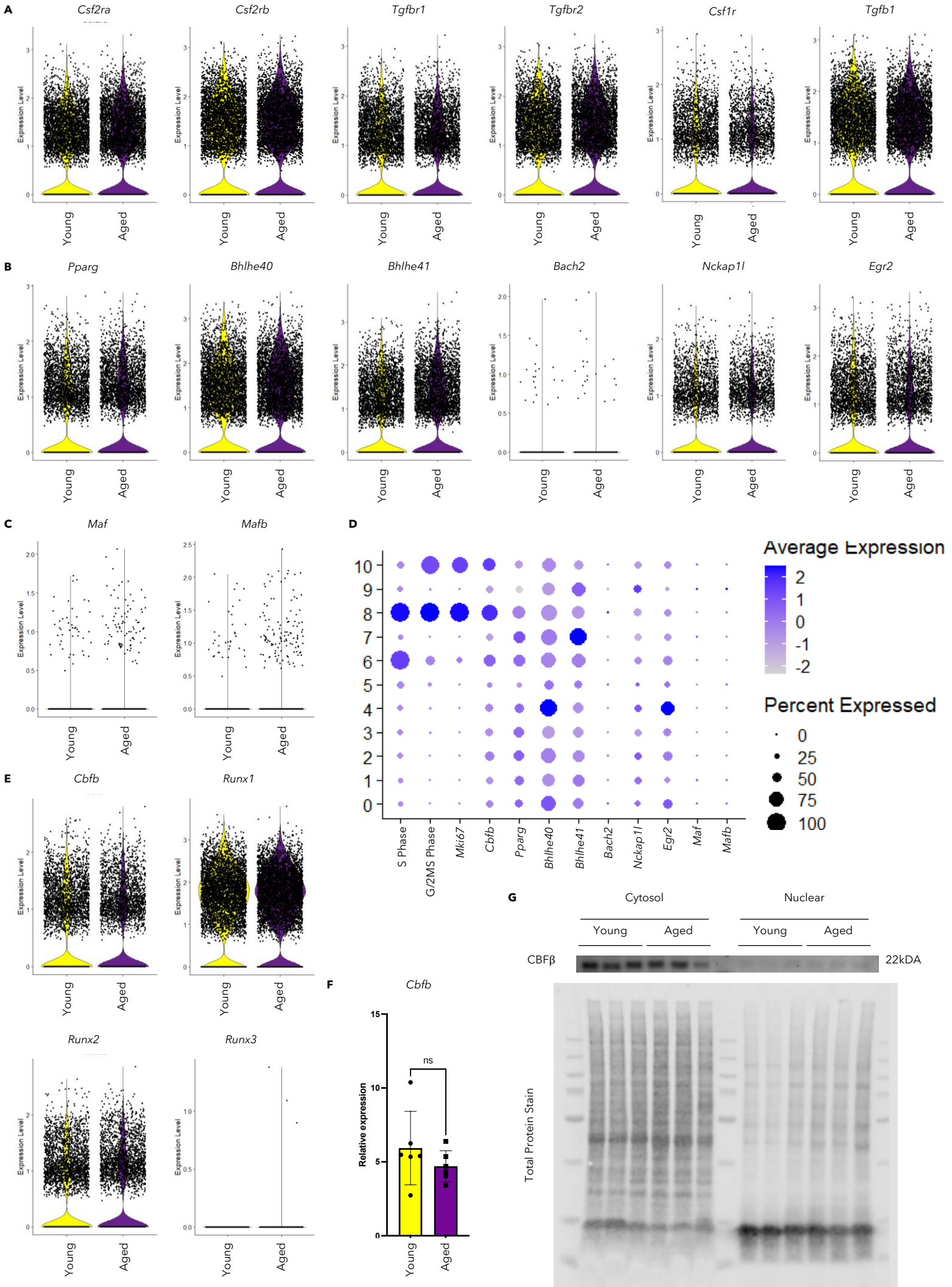

Figure S4 Characterization of proliferation related profile in AMs from young and aged mice, related to Figure4.

(A-E) Data are from scRNAseq of AMs from young and aged mice as shown in **Figure3. A.** Violin plots showing expression level of mRNA for GM-CSF receptors, TGF-β receptors, M-CSF receptor, and autocrine TGF-β. **B.** Violin plots displaying transcription factors associated with the proliferation and identity of AMs. **C.** Violin plots demonstrating mRNA level of transcription factors that suppress the ESC-like features of AMs. **D.** Dot plot revealing module scores for S-Phase or G/2M-Phase related genes, expression of transcription factors related to proliferation and identity of AMs, and expression transcription factors associated with the suppression of the ESC-like feature of AMs. **E.** Violin plots displaying mRNA level of *Cbfb* and RUNX family members (*Runx1*, *Runx2*, and *Runx3*). **F.** Quantification of relative mRNA level of *Cbfb* in AMs from young and aged mice using qPCR. Data were combined from 2 independent experiments. Each dot represents one biological replicate. **G.** Western Blotting of the bands for CBFβ **(top)** and total protein stain **(bottom)**.

Unpaired student t test with Welch's correction **(F)** was utilized for statistical evaluation. Data in **(D)** were displayed in dots with diameter representing the percent of cells in the cluster (as shown in **Figure 3B)** that expressed the gene (or list of genes) indicated, with the depth of color indicating the average expression level.

Supplementary Figure 5

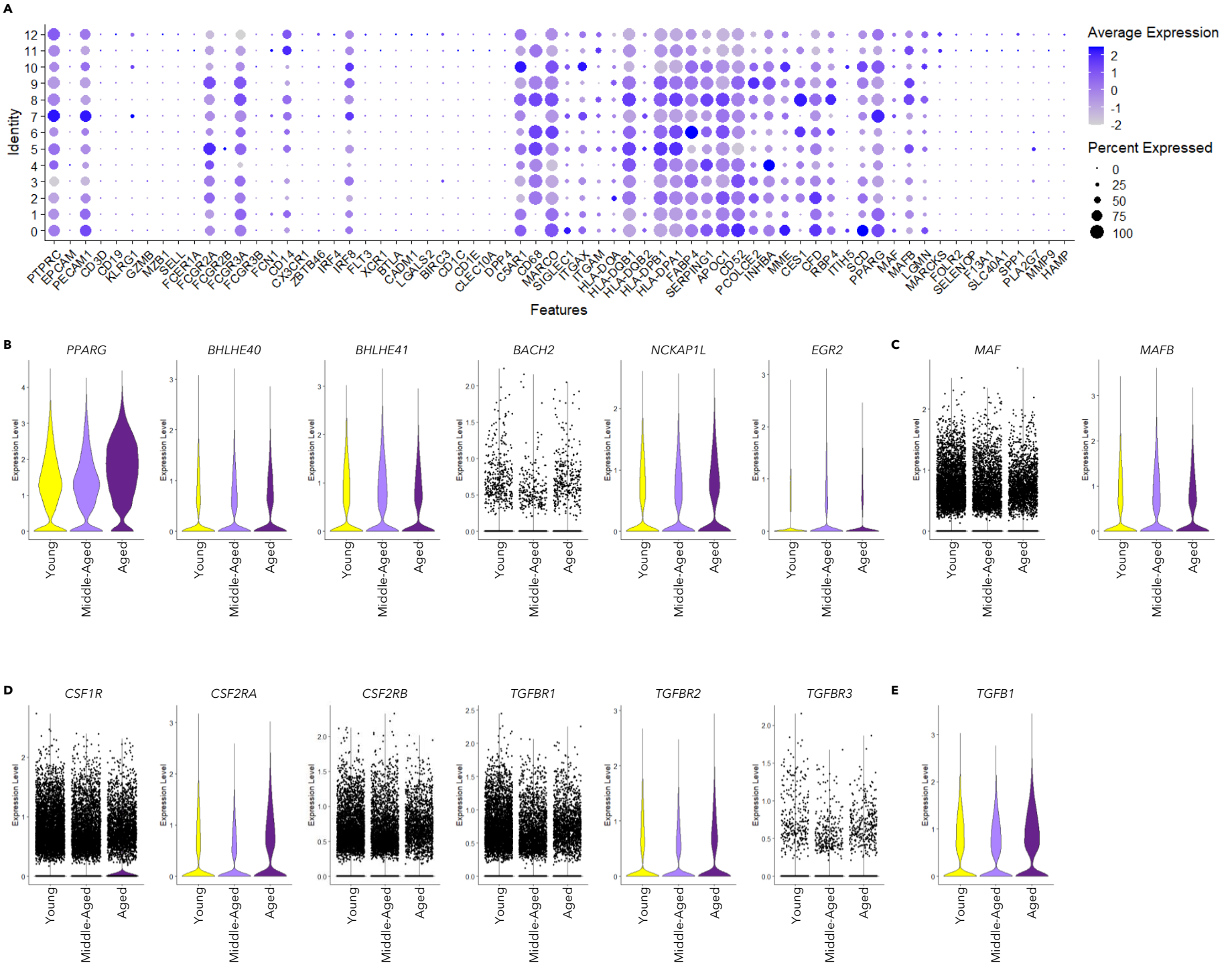

Figure S5 Characterization of proliferation related profile in AMs from human, related to Figure 5.

Data of human AMs were extracted from combined scRNAseq profiling pneumocytes of "Healthy" donors (GSE135893[52], GSE122960[53], GSE128033[54], GSE136831[55]). Samples were divided into "Young" (<40-years old), "Middle-Aged" (40-60- years old), and "Aged" (≥ 60-years old) groups. In total, 79 samples with 35 "Young", 27 "Middle-Aged" and 17 "Aged" were included. **A.** Dot plot showing markers for identification of AMs. **B.** Violin plots demonstrating mRNA level of transcription factors associated with the proliferation and identity of AMs **C.** Violin Plots manifesting transcription factors shown to inhibit the ESC-like features of AMs. **D.** Violin plots showing expression of mRNA for components of M-CSF receptor, GM-CSF receptor, and TGF-β receptor. **E.** Violin plots displaying mRNA level of autocrine TGF-β.

Data in **(A)** were displayed in dots with diameter representing the percent of cells in the cluster **(Figure 5A)** that expressed the gene indicated, with the depth of color indicating the average expression level.